48th AIAA Aerospace Sciences Meeting Including the New Horizons Forum and Aerospace Exposition
4 - 7 January 2010, Orlando, Florida

AIAA 2010-1393

Supersonic Bi-Directional Flying Wing, Part II: Conceptual Design of a High Speed Civil Transport

Daniel Espinal*, Hongsik Im†, Brian Lee*, Joanna Dominguez*, Hannah Sposato*, Daniel Kinard*, Ge-Cheng Zha‡

University of Miami
Dept. of Mechanical and Aerospace Engineering
Coral Gables, FL 33124
E-mail: gzha@miami.edu

Abstract

This report designs a supersonic passenger transport using a novel supersonic bi-directional (SBiDir) flying wing (FW) concept that achieves low sonic boom, low wave drag, and high subsonic performance.

For supersonic flight, the planform is designed to achieve optimum aspect ratio, span, and sweep angle to minimize wave drag. For subsonic mode, the airplane will be rotated 90° so that the side of the airplane during supersonic flight becomes the front of the airplane. The sweep angle of the LE at subsonic mode is significantly reduced and the aspect ratio is considerably increased by $(L/b)^2$ where L is the airplane length, and b is the span. This will allow the airplane to have high subsonic performance with short take-off and landing distance and low stall velocity due to low wing loading. The airfoil suggested is symmetric about the 50% chord location with both sharp leading edge (LE) and sharp trailing edge (TE). The whole 3-D configuration is symmetric about the longitudinal and lateral planes. As the demonstration of concept, the AOA=0° is selected as the low boom design point. A flat pressure surface of the airfoil used as the isentropic compression surface is employed to cancel the downward shock and sonic boom. Diminished take off noise will be achieved by attaining a low stall velocity and mounting the engines on the upper part of the airplane in order to shield the jet noise. A novel LE radial air injection to delay LE stall is suggested to avoid using the conventional LE slats system, which is heavy and complicated. The calculation shows that the 90° rotation can be done in 3 to 5 seconds with a very small centrifugal acceleration. The rotation transitional time will be short enough not to lose lift and the acceleration is so small that no passenger discomfort will be created. This design has the mission requirements of a cruise f Mach 1.6, a range of 2,000 nautical miles, a payload of 70 passengers and a take-off field length of 2,471 feet. The sonic boom overpressure propagated to ground was found to be 0.3 psf at AOA=0°.

---

* Undergraduate Student, Dept. of Mechanical and Aerospace Engineering
† Graduate Student, Dept of Mechanical and Aerospace Engineering
‡ Associate Professor, Dept. of Mechanical and Aerospace Engineering, Senior AIAA Member

1. Introduction

Supersonic civil transports have always been a topic of aircraft design engineers, scientists, and business professionals due to the potential to reduce inter-continental travel time. The Concorde, the first supersonic civil transport to carry passengers, ceased service in 2003 due to high operating costs. The prohibition of the Concorde's flight over most areas limited its commercial success. Since the Concorde's last flight, numerous supersonic transport programs have tried and failed to produce a transport for commercial service. However, the dream of travelers to fly at supersonic speeds has never stopped.

Supersonic transports (SSTs) have two major problems: efficiency and noise. The first factor that affects efficiency is the extra drag contribution during supersonic flight: the wave drag caused by the entropy increase of strong shock waves. Wave drag does not exist for subsonic airplanes and is not a serious problem for transonic flight due to the low supersonic Mach number. The second factor that affects efficiency is the large flight speed disparity between take-off/landing and cruise. At take-off and landing, the low flight speed requires a high aspect ratio and low wing sweep angle. High-speed cruise however requires the opposite characteristics. A compromise between low speed take-off/landing and high-speed cruise efficiency is required. Noise is an issue caused by the sonic boom that propagates to the ground from the shock waves created by the leading edges of a supersonic airplane and its components. A supersonic airplane cannot be economically and environmentally viable if the efficiency and noise problems are not resolved.

The flying wing and blended wing body concepts eliminate the non-lifting fuselage component of the conventional tube and wing configuration, so efficiency during subsonic flight is improved. However, the flight of a supersonic flying wing or blended wing body configuration for civil transport has not appeared, and the full conceptual study of such configurations is rarely seen.

The oblique flying wing (OFW) concept first proposed by Jones was intended for the development of supersonic flying wings.[1,2] An excellent review of oblique wing history is given by Hirschberg et al.[3] and a helpful introduction to oblique flying wings and their conceptual design is provided by Desktop Aeronautics.[4] The advantage of oblique flying wings is that the sweep angle can be varied during a flight mission for different Mach numbers to obtain a high aspect ratio at low speeds and a low aspect ratio at high speeds.[2,3,5] Such performance is appealing for supersonic airplane design.

However, there are some difficulties with oblique flying wing or oblique all wing (OAW) concepts. First, the configuration of an OFW is asymmetric about flight direction. The asymmetry of the configuration may create serious problems for stability and control, in particular at a high sweep angle.[5,6,7,8,9] Even though the modern fly-by-wire control system could significantly improve stability, it may come with increased drag penalty because an asymmetric configuration is not the selection of nature. All flying animals have symmetric bodies about the flight direction, which is an evolution of nature after millions of years.

Second, to accommodate sufficient headroom for passengers, the airfoil thickness must be high and the OFW airplane size will be usually very large. This is because an OFW stacks the airfoil to align with the low speed flight direction and form a high aspect ratio elliptic planform. Hence, the airfoil chord is short. This is very different from the regular flying wing concept with the airfoil aligned with the flight direction and a long chord length. The high thickness airfoil of an OFW would not be favorable for supersonic Mach number flight due to the large wave drag. The large airplane size would also create airport operating difficulties.[10]

Both McDonnell Douglas and Boeing conducted the oblique all wing conceptual design for low supersonic cruise flight at Mach number of 1.2-1.3. The conclusion was that the thickness requirement of an OAW creates a "fundamental conflict" with the aerodynamic efficiency.[11] Combined with other difficulties of oblique wings, McDonnell Douglas and Boeing dropped the OAW concept as a viable supersonic passenger transport.

In the 1970's, NASA[12], Boeing[13,14], and General Dynamics[15] conducted oblique wing studies for transonic and supersonic transports. Interestingly, none of them adopted the OFW configuration. Instead, they used tube-wing configurations accompanied by the wings implemented by the oblique wing. The oblique wing designs of NASA[12] and Boeing[13,14] were for supersonic cruise, and the General Dynamics[15] design was for high subsonic cruise at a Mach number of 0.95.

The Ames-Dryden-1 (AD-1) oblique wing supersonic airplane based on the final design of Boeing's oblique wing had flight-testing at low speed. It was found that the aircraft's asymmetry resulted in unusual trim requirements, asymmetric stall, and inertial coupling.[6] For example, the AD-1 required about 10^{O} of bank in order to trim the aircraft with no sideslip at 60^{O} wing sweep.

The most promising potential advantages of oblique wings seem to be the improvement of aerodynamic efficiency with variable sweep angle and aspect ratio at different speeds. Wintzer et al. recently indicated that a conventional configuration could reach the similar supersonic cruise efficiency of an oblique wing.[16] The significant advantage of an oblique wing configuration is a high aspect ratio at low speed take-off/landing. However, the oblique wing configuration does not have an inherent advantage in reducing sonic boom.

Studies performed by scientists including Jones, Seebass, and George have concluded that by implementing bluntness at the tip of the aircraft, shock boom will be minimized.[1,20,21] A blunt nose design creates a shock distribution in which the largest shock strengths are near the aircraft. This is caused by a gradual loss in intensity as the shock wave travels from the aircraft to the ground. Unfortunately, this design also implements substantial drag. A sharp nose design on the other hand is aerodynamically efficient but produces a much stronger shock at mid-field and far-field distances from the aircraft. However, McLean found that the pressure signature that reaches the ground from a long slender aircraft with minimal weight change will not fully develop into the far-field N-wave form.[17] Darden investigated nose-blunt relaxation as a compromise between the blunt nosed low-boom aircraft and sharp nosed low drag design.[18]

The Quiet Supersonic Platform (QSP) program sponsored by DARPA made remarkable progress in weakening the sonic boom of a conventional supersonic aircraft with tube-wing configuration.[22] The flight tests of F-5E aircraft reshaped by Northrop Grumman and based on the aero distribution rule suggested by George and Seebass in the 1960s shows a significant reduction of sonic boom strength.[23]

The Quiet Spike was a joint program with Gulfstream Aerospace and NASA Dryden Flight Research Center in which the concept of an extendable nose spike for sonic boom minimization was investigated.[24] In supersonic flight tests with a spike mounted on F-15B aircraft, the typical N-shaped pressure wave was reduced to a series of small shocks. However, this design is intended for a small civil transport carrying 8-14 passengers. Use of this concept to achieve the goal of a larger civil transport with 35-70 passengers is not feasible due to the much larger sonic boom that must be minimized.

Previous efforts have focused on either reducing sonic boom or improving aerodynamic efficiency for the supersonic airplane system. So far, there is no viable aerodynamic system concept for supersonic airplanes that can achieve both high aerodynamic efficiency and low sonic boom.

Zha[25,26,42,43] in December of 2008 suggested a novel supersonic bi-directional flying wing concept (SBiDir-FW) aimed at limiting sonic boom, minimizing wave drag, and improving subsonic performance. The SBiDir-FW concept is to combine the advantages of conventional symmetric airplane configurations for stability and variable sweep of oblique wing for high aerodynamic efficiency. In addition, the SBiDir-FW adopts an isentropic compression pressure surface configuration to cancel sonic boom and a leading edge (LE) injection flow control method to increase stall margin.

The fundamental concept of SBiDir-FW includes the following features: First, the airplane is a symmetric flying wing with a thin airfoil stacked in the cruise flight direction to achieve high supersonic aerodynamic efficiency and sufficient volume. Second, the wave drag is minimized by the thin airfoil and the lifting load distribution along the long length of the flying wing. Third, the pressure surface of the flying wing is an isentropic compression furface, which minimizes the shock wave propagating downward and the resulting sonic boom. Fourth, the flying wing will have two flight directions altered by 90^O to favor both supersonic cruise and low speed at take-off/landing. The flight planform direction is rotated by 90^O to change from a high sweep angle at supersonic speed to a low sweep angle at subsonic speed and vice versa. Thus, a high aspect ratio will be achieved at low speed and a low aspect ratio at high speed. Fifth, a novel active flow control method using radial flow injection at leading edge is suggested to delay the leading edge stall due to the sharp leading edge. This report applies the SBiDir flying wing (SBiDir-FW) concept to the design of a supersonic civil transport that achieves supersonic cruise efficiency, low sonic boom, and high lift for take-off and landing. For this design, the SBiDir-FW transport will carry 70 passengers at a cruise speed of Mach 1.6, at a cruise altitude of 60,000 feet, for a range of 2000 nautical miles.

2. Geometry[25,26,42,43]

The conventional supersonic airplane always has the dilemma to favor supersonic performance and penalize the subsonic performance or vice versa. The reason is that at supersonic speeds a high sweep wing with small cross-sectional area is preferred to minimize the wave drag. However, at subsonic speeds, a small sweep with high aspect ratio is preferred to have large lifting surface, high dynamic pressure, and small induced drag. This can be provided by the planform of SBiDir-FW shown in Figure 1. It can be observed that depending on the direction of flight, different aerodynamic characteristics are employed. For subsonic flight, a low sweep angle is present and a large span is available; for supersonic flight, the wing is highly swept and its span is short ensuring the aircraft will be completely inside the Mach cone and thus reducing wave drag further. For this design it was observed that a double-delta type of leading edge (LE) was favorable and that the use of sweep angles of 80^O and 60^O displayed proficient aerodynamic characteristics for supersonic cruise conditions. For simplicity, the point of change of sweep is located at one quarter the length of the aircraft as shown in Figure 1.

The ability of SBiDir-FW to accommodate to the different flight conditions is due to the symmetry it exhibits for each flight direction; hence, it is required of this concept to be accompanied by an airfoil that is symmetric about its half-chord point. Because of the condition of symmetry, the maximum thickness must be at the half-chord point as well. The shape selected for this design was, for the suction surface, a circular arc, and for the pressure surface, a flat plate, as depicted in Figure 2. This airfoil is the one used along the span of the wing when flying supersonic; therefore the maximum thickness line is the lateral (x) axis in Figure 1 for supersonic flight, and inherently the longitudinal (y) axis for subsonic flight. Because a thin airfoil is preferred for supersonic flight, the circular-arc airfoil was designed to have a thickness

equal to 3% of the local chord length. This 3% thickness was kept constant for the supersonic configuration throughout the span.

As the isentropic compression surface at AoA=0, the flat pressure surface of the airplane will cancel or minimize the downward shock which is responsible for sonic boom propagating to ground[43]. Even with the boundary layer displacement thickness effect on the pressure surface, the Mach waves are expected to be diverged without coalescence. At non-zero AoA, an isentropic compression pressure surface needs to be designed using characteristic method. Even though the design point of this airplane requires the AoA=1°, the isentropic compression surface is not designed for AoA=1° due to time constraint.

The sharp leading edge of the airfoil will further weaken any shock waves due to 3-D effect. The wave drag is expected to be significantly lower than that of the conventional tube-wing configuration and oblique wings that usually do not have a sharp LE and the conical shocks generated are full annulus. Therefore, by using the thin circular-arc airfoil section with a flat pressure surface, a low sonic boom and low wave drag can be expected.

The geometry of the airfoil was selected mainly thinking on the cruise section of the mission since it is there where most of the fuel consumption occurs and where the sonic boom propagation is most critical. Therefore, although the planform geometry was designed with both subsonic and supersonic flights in mind, the airfoil section geometry for the subsonic mode of the aircraft will rather depend on the LE shape of the wing. The subsonic airfoil sections vary in shape and thickness across its span as shown in Figure 3. Figure 4 presents the thickness distribution for both supersonic and subsonic modes. It can be observed that the thickness of this design ranges from 8% at the root (or axis of symmetry) to about 34% close to the wingtip for subsonic mode while it remains constant at 3% for supersonic mode.

At subsonic mode, the sharp LE may reduce the airplane stall margin. There are three ways to resolve this problem[43]. First, conventional airplane LE slats can be used to create the effect of a round LE. During supersonic cruise, the slat will be stored inside the airplane and extended outward during subsonic flight. The slat system requires moving parts, which introduces extra weight and system complications. The second method proposed is an innovative method of using radial air injection at the sharp LE as shown in Figure 5 (a). The aerodynamic principle is that a uniform flow superimposed with a source flow will create a blunt body flow as shown in Figure 5 (b). By adjusting the source strength, the effective LE radius (R) can be controlled. This will be a much simpler way to increase the LE effective radius in order to reduce LE stall. This technique can be used for all kinds of airfoils at subsonic and supersonic flight. However, it appears particularly useful for supersonic airfoils. Third, the sharp leading edge stall margin and lift enhancement may be achieved by using the delta wing detached leading edge vortices.

3. Computational Fluid Dynamics (CFD) Analysis[43]

After developing the geometry, the procedure followed to analyze the concept of SBiDir-FW was to first perform a CFD analysis to get the aerodynamic characteristics of the aircraft. Figure 6 and Figure 7 show the mesh generated to analyze the configuration dubbed “SB-8060-3” where SB stands for SBiDir-FW, 80 and 60 represent the sweep angles of the leading edge and 3 shows the circular-arc airfoil has a thickness of 3%. The mesh is H-type and is inclined to measure the sonic boom two body-lengths below accurately with the angle depending on the cruise Mach number. For this design the Mach number is 1.6 and therefore the angle of inclination is about 38.7^{O} which is the angle of the mach cone generated by the aircraft. The CFD analysis was only applied to the supersonic configuration. A future paper will present the CFD analysis for the subsonic configuration.

Because of the mesh type, it was found that the drag coefficient was being overestimated because the friction part was larger than what it should be; therefore, Figure 8 and Figure 9 are based only on the pressure drag coefficient. Figure 8 shows the results for lift coefficient (C_L) and pressure drag coefficient (C_{Dp}) for a range of angles of attack (AoA). The C_L for SB-8060-3 is comparable designs like the S3TD[27] (Silent Supersonic Technology Demonstrator). Figure 9 presents the L/D estimation using C_L/C_{Dp} with respect to AoA. The estimated L/D is close to 11 which is rather high for a supersonic transport, but it is expected that in real life this value be lower because of friction drag; thus, for further analysis of this design, a conservative L/D value of 7.5 is used which is lower than the values for typical supersonic transports and small business jets.

Figure 10 shows the isentropic Mach contours for the upper and lower surfaces at different AoA. A strong shock on the upper surface and a bottom surface that remains almost uniform is evident for every AoA analyzed. This demonstrates that the shock waves at the bottom of the circular-arc airfoil are not as strong as the ones at the top, which was expected from theory. Figure 11 further illustrates these findings with the distributions of pressure and flow Mach number around the aircraft. The implications of these phenomena towards sonic boom propagation are presented at a later section in this paper.

4. Conceptual Design

Corke's Design of Aircraft[28] provides an excellent aircraft conceptual design methodology that was modified for the SBiDir-FW design. A FORTRAN code was written based on this methodology in order to facilitate iterations. Using the initial constraints, a preliminary estimate of the aircraft weight at different flight stages was made by using standard estimates of the weight of passengers and crew, luggage, cockpit, engines, and other components. Once weight was calculated, a selection of the overall length (see Figure 1) was performed. The constraints that mostly affected the selection of the length were the maximum height of the aircraft reached by this length (i.e. max. height is 3% of the overall length), the volume made available by this configuration and the C_L required to lift this configuration.

In this design, the SBiDir-FW configuration is expected to provide a very low wing loading, and thus short take-off and landing distances are expected. To choose the propulsion system, a computation of the overall aircraft drag is performed to ensure that the plane has sufficient thrust, and then engines that meet the thrust requirements are chosen.

4.1. Preliminary Take-off Weight Estimate

The take-off weight consists of fuel weight, payload weight, and empty weight. The fuel weight is mostly dependent on the fuel consumption of the engine selected for the range of the mission. The payload weight refers to the cargo such as passengers and luggage and the empty weight refers to the structural weight of the airplane.

For the cruise out to destination flight phase, the range constraint is 2000 nautical miles and is defined for a turbojet engine as:

$$R = \left(\frac{V}{TSFC}\right)\left(\frac{L}{D}\right) ln\left[\frac{W_i}{W_f}\right]$$

where V is the cruise velocity, L is the lift, D is the drag, TSFC is the thrust-specific fuel consumption, and W_i/W_f is the ratio of initial weight to final weight of the flight phase.

A finalized weight estimate is provided in Table1. The maximum take-off weight of 81 Klb is less than that of the Concorde[29] (408 Klb). The lower take-off weight is expected due to the lower passenger payload and higher aerodynamic efficiency. The TSFC for the proposed reference engine, F118-GE-100, is approximately 0.70. Fuel consumption is higher during supersonic flight. The Concorde[29] had a TSFC of 1.2 lb/(lbf hr) and turbojet engines at supersonic speeds had a TSFC range of 1.06-1.77 lb/(lbf hr) in a 2001 engine performance paper by Liu and Sirignano.[30] A TSFC of 0.8 lb/(lbf hr) was assumed for the engine selected at Mach 1.6. The passenger weight including baggage is assumed to be 250 lbs for a total payload of 17.5 Klb. The flight altitude selected for cruise is 60,000 feet, which is the same altitude of the Concorde.[29]

The estimated fuel weight is required for the mission is 27.2 Klb. This fuel estimation includes the fuel required for take-off and landing, for climbing and accelerating to cruise conditions, cruising to destination, 15 minutes of loiter time before landing, an estimated 5%of fuel reserve and an estimated 1% of trapped fuel. For 70 passengers covering a range of 2,000 nm, a fuel efficiency of 5.93 passenger-miles per pound of fuel is calculated. A structure factor of 0.45 was selected resulting in an empty weight of 36.6 Klb for SB-8060-3.

After reaching the cruising altitude and beginning to cruise at a constant speed, the aircraft is estimated to weight 74.6 Klb. The planform area of the wing for a length of 60 m is 494.5 m^2, which means that, to maintain SB-8060-3 at level cruise, a C_L of about 0.06 is required. This C_L is very close to the one calculated for an AoA of 1^O in the preliminary CFD analysis. Therefore it can be concluded that a length of 60 m fits well the aerodynamic characteristics of SBiDir-FW. Since a value of 7.5 was assumed for L/D the C_D can be found to be about 0.008, and for cruise conditions a total drag of 9,950 lbs was calculated.

4.2. Volume Considerations and Cabin Layout

Passenger requirements are the primary factor for volume. A capacity of 70 passengers is chosen. Typical values of seat width, seat pitch, headroom, lavatories per passenger, and other compartment requirements are used. A comfortable flying experience is desirable. Thus, rotating seats with adequate leg room are factored into the volume estimation. Due to the novel shape of the SBiDir-FW design and its configuration change, conventional aisles will not be convenient for passenger comfort. Instead, groups of seats will be placed according to their class. 70 coach class seats will be placed in the center of the cabin where sufficient headroom is available. Drawings of the interior layout are provided in Figure 12 and Figure 13.

The maximum height of the cabin is 1.8 m and the minimum height is 1.4 m. There is only one class where the maximum height of the seat is 1.2 m and the width of the seat is 0.5 m. The seats were placed along the middle of the airplane, where less g-forces are felt by the passengers during mode change of the aircraft. The seats are in columns of 2 and 3 as shown in Figure 12 and Figure 13.

There are four bathrooms as well as an area for the flight attendants. The flight attendants have seats similar to those of the passengers, but they do not have recliner capabilities. Aisles are not necessary for the SBiDir-FW design since there is a spacing of 0.675 m between each seat. The spacing is due to reclining capabilities of the passengers' seats as well as room for the rotation of the seats when changing from subsonic to supersonic mode and vice versa. The required volume of the cabin was calculated to be approximately 110 m^3. The CAD program used, Pro-E Wildfire, calculated the available volume of the

passenger cabin to be approximately 116 m^3 as shown in Figure 13. This is sufficient for the volume required of the cabin interior.

The pilot and co-pilot board the SBiDir-FW aircraft in the same manner that a pilot boards a fighter jet. The window covering the cockpit will raise and the pilot will board with the aid of stairs. The pilots will then lie down. The window will close and lock. The maximum height of the cockpit is 0.6 m and the minimum height is 0.4 m. Therefore, since space is limited, the pilots will always be in a lying down position. The cockpit was designed so the pilot seats can move along a track. During take-off and landing, the pilots will be towards the front of the cockpit. Visibility will not be distorted or blocked since the pilots are close to the front of the aircraft. During cruise, the pilots will be able to move (slide) their seats to the back of the cockpit where more head room is available. The pilots will still be in a lying down position, but they will be comfortable since there will be more space to move around.

From the weight estimation section, a fuel weight is calculated. Using the specific volume of AV-gas at $100^{O}F$, a required fuel volume is found to be 22.6 m^3. A common tricycle landing gear configuration is chosen. For the subsonic configuration, one nose gear is in the front of the plane, and two main gears are in the back. Each main gear has three wheels, and the nose gear has two wheels. Knowing this information, a landing gear volume of 1.54 m^3 is required. Therefore adding all of the volume requirements will yield a total volume required of 140 m^3 without taking into account the volume for cargo and cockpit. Since the total available volume is calculated to be 328 m^3 for SB-8060-3, it is assumed that there is enough volume for cargo, cockpit and any extra systems required like piping for LE treatment and rails for engine rotation.

4.3. Engine Selection

In order to choose an appropriate propulsion system to power the aircraft, the required thrust must be known. To determine how much thrust is needed, a reference airliner was used. The Concorde airplane was chosen as the reference aircraft because its specifications are comparable to the design criteria. The Concorde uses four Rolls-Royce/Snecma Olympus 593 turbojets at 32,000 lb of static thrust each, giving a total thrust of about 128,000 lb for operation[29]. Based on the lower payload and higher aerodynamic efficiency, the SBiDir-FW will require a lower total thrust than that of the Concorde. An initial estimate of 80,000 lb of total thrust from two engines is made for the SBiDir-FW. The other requirements for the engines include 1) low-bypass ratio for sound reduction and low drag during cruise and 2) a low dry weight to reduce the necessary lift. Searching through all of the low-bypass engines, the General Electric F118-GE-100 turbofan used to power the B-2A Spirit stealth bomber was chosen as the reference engine. The F118-GE-100 has a bypass ratio of 0.87, 19,000 lb of dry thrust, and a weight of 3,200 lb. A turbojet engine is the best option for supersonic flight and would be used for a SBiDir-FW prototype. However, the current engines produced by major engine manufacturers are only turbofans, so a low-bypass engine, the F118-GE-100 turbofan, is used. Because the maximum thrust for this reference engine is lower than that needed, a sizing factor of 1.66 was employed to bring the thrust up to the required amount. Each scaled engine has a thrust of 31,446 lb and weighs 3,806 lb. The SBiDir-FW propulsion system is composed of two engines for a total thrust at sea level of 62,893 lb with an installed weight of 9,897 lb. These engines will have a diameter of 59.8 inches and a length of 129.3 inches with a mass flux rate of 475 lb per second each. These dimensions are reasonable when compared to the overall length of 60 m (or 197 feet). Also, the engines will be mounted on the upper surface of the aircraft in order to minimize the engine jet noise at take-off by shielding the noise emitted from propagating to the ground. The shock

waves generated by the engines during supersonic flight will also be blocked by the aircraft preventing the shock propagation to ground. There will be a small distance between the engines and the airplane surface to avoid interrupting the flying wing flow.

4.4. Wing Loading

Wing loading affects several aspects of flight, namely the stall velocity and the turn rate of the aircraft. Wing loading varies during the mission as the aircraft weight changes. The SBiDir-FW has a low maximum wing loading of 15.3 lb/ft^2 due to its improved aerodynamic performance and large planform area, characteristics inherent in flying wings. From flight dynamics it is known that the lower the wing loading the lower the stall velocity. Because of this, having a lower stall velocity will require significantly shorter runway length for takeoff and landing. This aircraft exhibits a stall velocity at takeoff of 112.8 ft/s.

The load factor, which will influence the maximum sustained and instantaneous turn rate of the aircraft, is also affected by the wing loading. Also from flight dynamics it is known that the lower the wing loading, the higher the load factor the aircraft can sustain, which in turn will reciprocate on the maximum turn rate that the aircraft can undergo. The maximum calculated load factor for this aircraft is 4.02 with a maximum calculated sustained turn rate of 7.56^O per second before cruise and 9.92^O per second after cruise. These values are calculated for a flight Mach number of 0.8 at a height of 60,000 ft which corresponds to the flight conditions immediately before the aircraft changes from subsonic to supersonic mode.

4.5. Runway Length

The runway length is calculated for take-off and landing. The take-off runway length is the sum of the lengths for each step of the take-off process. The landing runway length is calculated in the same manner. The Federal Aviation Regulations (FAR) included in the Code of Federal Regulations (CFR) sets the minimum take-off specifications depending on the type of aircraft and aircraft engines. For simplicity, the following values employed by Corke are used[28]

$$V_{TO} \geq 1.1V_s$$
$$V_L \geq 1.3V_s$$

where V_{TO} is the take-off velocity, V_L is the landing velocity, and V_s is the stall velocity.

The take-off phases are ground roll, rotation, transition, and climb. In ground roll, the aircraft accelerates from rest to take-off velocity. In rotation, the aircraft AoA increases to 80% of the maximum lifting coefficient. The aircraft velocity during rotation is the take-off velocity, and the rotation time is assumed to be a typical value of three seconds. In transition, the aircraft flies along a circular arc. The height at the end of transition is achieved when the climb angle is reached. Climbing begins after transition and ends when the aircraft reaches a certain obstacle height, which is 35 feet for commercial aircraft. After summing the lengths of each phase, the take-off length is found to be 1,827 feet.

The landing phases are approach, transition, free-roll, and braking. During approach, the aircraft descends at constant velocity from a height of 50 feet to the transition height. In transition, the aircraft flies along a circular arc while the aircraft velocity decreases. During free-roll, the aircraft flies at a constant velocity. The free-roll time is assumed to be three seconds by convention. Braking is the deceleration of the plane on the runway, and is governed by the take-off ground roll equations. After summing the lengths of each phase, the landing runway length is found to be 2,471 feet.

The take-off length and the runway length are compared. The higher value governs, so the minimum take-off runway length is 2,471 feet. The low stall velocity of the SBiDir-FW allows for and extremely short take-off and landing (ESTOL) runway length, which makes take-off and landing at major airports and the majority of regional airports feasible.

4.6. Stability and Control

The intent of this section is to explain the method in which the control surfaces will control the six degrees of freedom of the SBiDir-FW and rotation for mode change from subsonic to supersonic and vice versa.

Figure 14 shows the placement of four flaps on SBiDir-FW, two for subsonic control and two for supersonic control. The description on how the flaps should be used applies for both subsonic and supersonic mode. Therefore, the description on how each type of motion is achieved will only refer to two flaps, which are the two activated flaps for the mode under which the aircraft is flying.

Figure 15 shows a special split flap, which is the type of control surface that will be used along the trailing edges of the wing for both subsonic and supersonic mode. It should be noted that this split flap is not the one commonly defined in the literature. The split flap proposed in this case has a top and a bottom section, each with the capability to move independently of the other section. Each section moves independently in order to compensate for the lack of a vertical stabilizer (i.e. rudder) in this design. This type of flap is similar to the split rudder of the Space Shuttle which acts as a speed brake.[31] This type of response is the one desired to control yaw without affecting pitching or rotation. Therefore, SBiDir-FW is required to use a state-of-the-art fly-by-wire control system due to the complexity of the use of the control surfaces.

As of now, only two split flaps will be required for each mode where each flap will be placed on both sides of the wing like a usual aircraft wing. Therefore, a total of four flaps must be placed on the SBiDir-FW for full motion control. Only the two corresponding flaps for each mode will function at their corresponding mode and the other two flaps will be locked and unavailable.

The first type of motion to be addressed is pitching. To control pitch, the flaps on both sides of the wing must be used in the following manner: to move the nose up, only the top portion of both flaps on the wing must be used; to move the nose down only the bottom portion of both flaps must be used. To control yaw, the following procedure must be used: to turn counterclockwise, both top and bottom of only the flap to the left of the flying direction must be used; to turn clockwise, both top and bottom of only the flap to the right of the flying direction must be used. Ultimately, rolling is achieved by the following system: looking from the front towards the back, to rotate counterclockwise (left roll), only the bottom of the flap to the left of the flying direction and only the top of the opposite flap must be used; to rotate clockwise (right roll), only the bottom of the flap to the right of the flying direction and only the top of the opposite flap must be used. While this is a simplistic description on how to maneuver SBiDir-FW, fly-by-wire controls must make up for the other aerodynamic moments affecting the motion desired. The above short description on how to maneuver the SBiDir-FW is standard, yet sufficient to understand how to perform basic maneuvers.

In order to improve the aerodynamic efficiency of the aircraft in subsonic flight, winglets will be created by bending a small section of the wingtips for the subsonic mode. The winglets will be activated to a near-vertical position only during subsonic flight. This feature will reduce the lift-induced drag of the aircraft and improve overall subsonic aerodynamic efficiency. Controls will cause the winglets to

deactivate and revert to a horizontal position flush with the wing when needed in preparation for supersonic flight. This deactivation will be complete before the rotation to supersonic mode is initiated so that aerodynamic issues during the mode change are minimized.

Two canards, one on each side of the front of the aircraft close to the nose, will be activated during supersonic flight. They will serve as horizontal stabilizers for longitudinal control and stability. The main advantage of the canard configuration is that it acts to counter the pitching moment generated by the main wing while being used as a lifting surface, therefore improving overall aerodynamic efficiency.

Vertical tails are typically used for stabilization. However, their usage should be avoided for the SBiDir-FW aircraft because there would be a drag penalty. Alternatives that can be used to improve stability and control include vortex flow control and thrust vectoring. The X-29 aircraft, a joint venture between NASA and Northrop Grumman, employed two nozzle jets on the forward upper part of the aircraft nose for vortex flow control.[32] In the 60 tests that were conducted, the results showed that higher-than-expected yaw forces were created. The process is as follows: Air is exhausted through the right nozzle to accelerate the right vortex flow. The left vortex is then pushed away from the body. As a result, there is a lower pressure on the right side of the body, which causes a right yawing motion of the aircraft. Thrust vectoring has been employed in fighter jets to achieve better maneuverability. This concept employs mechanical parts to rotate nozzles. The nozzles rotate, which affects the direction of the exhaust. With this capability, the aircraft does not have to rely solely on the control surfaces such as flaps to facilitate movement. A current field of research is flow thrust vectoring that uses injection nozzles.[33] With this system, flow is injected to control the exhaust vector. The flow thrust vectoring system does not require mechanical parts, so it is simpler and lighter than a typical thrust vectoring system.

The stability and control of the SBiDir-FW concept is a challenge. Ideas to stabilize and control the aircraft have been proposed. Stability and control during mode change of the SBiDir-FW is a primary concern. Analysis of stability and control derivatives over a range of flight conditions including the mode change should be conducted to determine the physical feasibility of the bi-directional flying wing concept.

4.7. Mode Change

The operation for yawing control is applicable to the mode change from subsonic to supersonic and vice versa. Transition refers to the rotation of the direction of the thrust relative to the planform. To achieve this there are two options: to turn the engines through a mechanical system, or by using the aerodynamic forces on the wing to rotate the airplane under the engines. The latter is preferable since it is the most energy efficient method.

In order to ensure that the engines only rotate 90^{O}, two ideas are proposed. The first is that the engines will be mounted on a circular platform with a raised cross at right angles. Each leg of the cross will be positioned between two panels to prevent unwanted rotation. A mechanism will be employed to remove both panels leaving the circular base to rotate freely. As soon as the leg clears the path of the panel, the right panel (counter clockwise rotation) or the left panel (clockwise rotation) will be replaced. Once the next leg reaches the replaced panel it will be prevented from moving further and the other panel will be put back locking the leg in place and ensuring a rotation of only 90^{O}.

The second idea is to employ an electromagnetic system that prevents the circular disk from moving when employed but leaves it free to rotate when disabled. The system can be hooked up to a computer that is programmed to know when the wing is in the correct position. The system will release the disk and

allow it to rotate freely while it gradually increases the strength of the magnetic system, eventually bring it to a stop when the wing has rotated 90^{O}. Either system or a combination of both systems can be employed to ensure proper rotation from subsonic to supersonic mode, and vice versa.

SBiDir-FW has been designed so that a counterclockwise turn is performed to change from subsonic to supersonic mode. Similarly, to change from supersonic to subsonic mode a clockwise turn must be executed. The time required for the transition between modes is estimated to be about 3.1 to 5.5 seconds. This time appears to be short enough so that from an inertia point of view neither momentum nor lift should be affected. Considering the effect of the transition on the passengers' comfort, for the chair furthest from the axis of rotation (about 11 m) a maximum centrifugal acceleration of 0.3g is felt, which is comparable to that felt at the transition phase of take-off (approx. 0.15g). As a result, passenger discomfort is not expected.

For transitioning onto supersonic mode, it is required that several conditions be met before the engines are allowed to rotate freely. First, SBiDir-FW must be in a level flight at a height of 60,000 ft which is the height for cruise. Second, a constant Mach number of about 0.8 must be reached. The engines must produce a constant thrust while the wing rotates under the engines. Only after the transition has been fully completed should the aircraft be accelerated to cross the sound barrier. Transitioning back to subsonic mode has the same requirements.

4.8. Material Selection

When flying at supersonic speeds, the outer surface of an aircraft has extremely high temperatures that can weaken the aircraft. For a cruise speed of Mach 1.6, the approximate maximum temperature is below $100^{O}C$[34], so materials that can withstand high temperatures are desirable. The weight and cost of a material is also a key consideration. A lighter material results in a greater payload and better fuel efficiency.

Aluminum is the most frequently used material for aircraft structures. It exhibits good mechanical and thermal properties and is relatively cheap. The most commonly used aluminum alloy is Duralumin, Al 2024. Some metal alloys including titanium and stainless steel have the required thermal and mechanical properties for a cruise speed of Mach 2.0. However, metal alloys are heavy which negatively affects the performance of the aircraft. In addition, their performance at slightly higher speeds (higher temperatures) is not acceptable.

In the literature, composite materials are commonly chosen for aircraft structures due to their light weight and good thermal and mechanical properties. Composite materials consist of a matrix (resin) and fibers. Epoxy resin is the most commonly used and has a maximum temperature limit of $180^{O}C$.[28] Due to the need for a factor of safety the actual temperature limit for usage is about $130^{O}C$, above the approximate maximum temperature for the SB-8060-3 outer surface. Typical fiber materials include graphite, aramid, boron, and fiberglass. Graphite is the most popular material for primary structures, and fiberglass is generally used for secondary structures. Composites cost more than metal alloys, so a combination of materials including various composites and metal alloys must be used to satisfy performance and cost concerns for the SBiDir-FW. For example, a graphite-epoxy composite can be used for the highest temperature areas of the aircraft, but it costs about 20 times more than aluminum. As a result, composite materials cannot be used for the entire airplane structure. Metal alloys should be used for areas where the conditions do not require composites in order to balance the cost and weight

considerations. To select specific materials for each part of the aircraft, a heat transfer analysis of the surface of the aircraft is needed.

5. Sonic Boom Analysis[43]

The CFD analysis provides an output result for the near-field overpressure (two body lengths below the aircraft). Using this overpressure value, the sonic boom can be extrapolated to determine the overpressure on the ground. The NFBOOM sonic boom extrapolation and sound-level prediction code was employed for this purpose.[35,44] The NFBOOM code is based on previous work developed by various NASA scientists. This includes the extrapolation of sonic boom pressure signatures by the waveform parameter method and without the use of a Whitham F-Function.[36,37] One subroutine adds a rise time amount to all shock waves in the pressure signature.[38] The NFBOOM results have very good agreement with another extrapolation and sound-level prediction code created by Wyle Laboratories called MDBOOM[39].

The overpressure plot in Figure 16 shows the ground N-wave signature of SBiDir-FW at angles of attack from 0^O to 4^O with the reflection factor of 1.9. This factor represents the reflection of the sonic boom due to the ground effect. The literature shows that the overpressure calculated for an altitude of 0 feet without change in medium density (no ground) differs from that measured on the ground by a factor between 1.9 and 2.0.[40,41] The overpressure for SBiDir-FW calculated by NFBOOM is about 0.3 psf at AoA=0° and 0.9 psf at AoA=1° for an angle of attack of 1^O, which is the requited cruising angle of attack to provide the L/D. The sonic boom signature at AoA=0° is also a smooth *sin* wave shape instead of the typical N wave shape with two shock pulses. It demonstrate that it is indeed possible to cancel sonic boom by employing the SbiDir-FW configuration with isentropic compression pressure surface[**43**]. This overpressure is much lower than that of the Concorde, which is 1.94 psf. The reason that the sonic boom is higher at AoA=1° is primarily because the flat surface is an isentropic compression surface only for AoA=0° , not for AoA=1°. Future work will design the isentropic compression surface for AoA=1° in order to reduce the ground sonic boom to the level of 0.3psf.

6. Final Configuration Summary

Table 2 shows a comparison between the dimensions of the baseline Concorde and SBiDir-FW final dimensions. Table 3 provides a comparison between Concorde and SBiDir-FW in performance characteristics showing a faster Concorde with a larger range but a quieter SBiDir-FW that is more fuel efficient and requires a significantly smaller runway length.

Because of the way the aircraft is defined, the maximum height becomes the thickness of the circular-arc airfoil, and the total length becomes the airfoil's chord length for supersonic configuration. This allows for several airfoil characteristics to be defined. Due to the required symmetry of the planform shape, the thickness to chord ratio varies. The center airfoil thickness is 3% in supersonic mode. When flying in a subsonic configuration, the airfoil chord length is the wingspan, so the center airfoil thickness is 8% of the chord length but has the same absolute value as in supersonic mode. A comparison of geometric characteristics between modes is shown in Table 4. Figure 17 presents a final assembly drawing and Figure 18 shows an artistic rendering of the SBiDir-FW concept.

7. Future Work and Optimization

While this paper attempts to cover as much ground as possible, further work is required starting from CFD analysis of the subsonic configuration which is more complex due to the required LE treatment to prevent an early stall margin. A more detailed design of the control surfaces and testing is required to present a more practical supersonic transport. Further calculations must be performed to determine the static margin of SB-8060-3 with and without canards for both subsonic and supersonic modes.

While there is still more analysis to be done to areas that have not been tested, even further optimization must be performed to the areas that have been thoroughly analyzed as well since with every further analysis made more discoveries are uncovered. The main area in which research is being done is in the optimization of the airfoil section shape where the suction surface and the pressure surface are being changed to achieve a near-zero sonic boom during cruise and an improved aerodynamic efficiency (i.e. increase L/D). Further optimization of the planform is also necessary to obtain a maximized aerodynamic efficiency for both flight modes so that range may be increased as well as speed. The factors to be optimized include sweep angles, aspect ratio, airfoil section, isentropic compression pressure surface, suction surface spanwise shape, engine location and integration, etc.

Also a closer study of this concept for different applications should be performed such as hypersonic vehicles or unmanned aerial vehicles (UAV). The possibilities of application are rather substantial due to the fact that quiet and efficient supersonic flight is required to continue on the evolutionary process of flying man-made structures, and the SBiDir-FW may be the answer to these issues.

8. Conclusion

A conceptual design of a supersonic commercial transport was designed for a capacity of 70 passengers for a range of 2000 nautical miles and a cruise speed of Mach 1.6 using the Supersonic Bi-Directional Flying Wing (SBiDir-FW) concept. A low sonic boom was achieved when compared to other supersonic commercial aircraft, with a ground overpressure of about 0.3 psf at AoA=0° with isentropic compression pressure surface and 0.9 psf at AoA=1° which does not have an isentropic compression pressure surface. A high fuel efficiency of 5.93 passenger-miles per pound of fuel is calculated while assuming that the power plant to be used will have a TSFC of 0.8 lb/(lbf hr) for the design cruise Mach number. An ESTOL runway length of 2,471 feet was found for this design.

While further refinements are required of this concept, SBiDir-FW has shown great promise by achieving a low sonic boom at the ground at a very early stage of its conception. The conceptual design of SB-8060-3 has been developed confirming its feasibility for future application as a tool to open the possibility of supersonic flight to the aviation industry. This design has shown improved performance over previous transports while still having room for further development.

9. References

[1]Mack, R. J., and Needleman, K.E., "A Methodology for Designing Aircraft to Low Sonic Boom Constraints," NASA TM-4246, February 1991.

[2]Jones, R. T., "Aerodynamic Design for Supersonic Speeds," *Proceedings of the 1st International Congress in the Aeronautical Sciences (ICAS), Advances in Aeronautical Sciences*, Vol 1., Pergamon Press, NY, 1959.

[3]Hirschberg, M., Hart, D. and Beutner, T., "A Summary Of A Half-Century of Oblique Wing Research," AIAA Paper 2007-150, 2007.

[4]"Oblique Flying Wings: An Introduction and White Paper," Desktop Aeronautics, Inc., Stanford, CA: June 2005. http://www.desktopaero.com/obliquewing/library/whitepaper/index.html

[5]Campbell, J.P., and Drake, H.M., "Investigation of stability and control characteristics of an airplane model with a skewed wing in the Langley free flight tunnel," NACA TN-1208, May 1947.

[6]Matthews, H., "Oblique Wing Research Aircraft NASA AD-1," *World X-Planes Magazine*, No. 2, 2005.

[7]Kroo, I.M., "The Aerodynamic Design of Oblique Wing Aircraft," *Proceedings of the AIAA/AHS/ASEE Aircraft Systems Design and Technology Meeting*, CP 86-2624, AIAA, Washington D.C., 1986.

[8]Kennelly, R.A., Carmichael, R., Strong, J., and Kroo, I.M., "Transonic Wind Tunnel Test of a 14% Thick Oblique Wing," NASA TM-102230, Aug. 1990.

[9]Kempel, R.W., McNeill, W.E., and Maine, T.A., "Oblique-Wing Research Aircraft Motion Simulation with Decoupling Control Laws," AIAA Paper 88-402, 1988.

[10]Jones, R.T., "Technical Note – The Flying Wing Supersonic Transport," *Aeronautical Journal*, Mar. 1991.

[11]Rawdon, B.K., "Oblique All-Wing Airliner Sizing and Cabin Integration," AIAA Paper 975568, 1997.

[12]Jones, R.T., U.S. Patent 3,737,121, filed 9 Dec. 1971.

[13]Kulfan, R.M., Neumann, F.D., Nisbet, J.W., Mulally, A.R., Murakami, J.K., Noble, E.C., Mcbarron, J.P., Stalter, J.L., Gimmestad, D.W., and Sussman, M.B., "High Transonic Speed Transport Aircraft Study," Boeing Commercial Airplane Company, NASA-CR-114658, 1 Sep. 1973.

[14]"Oblique Wing Transonic Transport Configuration Development, Final Report," Boeing Commercial Airplane Company, NASA CR-151928, Jan. 1977.

[15]Black, R.L., Beamist, J.K., and Alexander, W.K., "Wind Tunnel Investigations of an Oblique Wing Transport Model at Mach Numbers between 0.6 and 1.4," Convair Division of General Dynamics, NASA CR-137697, July 1975.

[16]Wintzer, M., Sturdza, P., Kroo, I., "Conceptual Design of Conventional and Oblique Wing Configurations for Small Supersonic Aircraft," AIAA Paper 2006-930, Jan. 2006.

[17]McLean, F. E, "*Some Nonasymptotic Effects on the Sonic Boom of Large Airplanes*," NASA TN D-2877, 1965.

[18]Darden, C. M., "Sonic-Boom Minimization With Nose-Bluntness Relaxation," NASA TP-1348, January 1979.

[19]Darden, C. M., "Minimization of Sonic-Boom Parameters in Real and Isothermal Atmospheres," NASA TN D-7842, March 1975.

[20]Jones, L.B., "Lower Bounds for Sonic Bangs," *Journal of the Royal Aeronautical Society,* Vol. 65, No. 606, June 1961, pp.433-436.

[21]Seebass, R, and George, A.R., "Sonic-Boom Minimization," *Journal of the Royal Aeronautical Society of America*, Vol. 51, No. 2, Pt. 3, Feb. 1972, pp. 686-694.

[22]Graham, D., Quiet Supersonic Platform, Shaped Sonic Boom Demonstrator (SSBD) Program, FAA Civil Supersonic Aircraft Workshop, Nov. 2003.
http://www.aee.faa.gov/Noise/aee100_files/SonicWkshp/2-Panel1-Graham-Northrop.pdf

[23]George, A.R., Seebass, R., "Sonic Boom Minimization including Both Front and Rear Shocks," *AIAA Journal*, Vol. 9, No. 10, 1971, pp. 2091-2093.

[24]Freund, D., Howe, D., and Simmons, F., "Quiet Spike Prototype Aerodynamic Characteristics from Flight Test," AIAA Paper 2008-125, 2008.

[25]Zha, G.-C., "A Supersonic Flying Wing with Low Sonic Boom, Low Wave Drag, and High Subsonic Performance (SFW-L^{2}HSP)," Technology Transfer Office UMI-163, University of Miami, Coral Gables, FL: Dec. 2008.

[26]Zha, G.-C., "Supersonic Bi-Directional Flying Wing," Provisional patent application No. 61172929, Submitted to USPTO, 27 Apr. 2009.

[27]Ishikawa, H., Makino, Y., Ito, T. and Kuroda, F., "Sonic Boom Prediction Using Multi-Block Structured Grids CFD Code Considering Jet-On Effects," 27th AIAA Applied Aerodynamics Conference, San Antonio, Jun. 22-25, 2009, AIAA-2009-3508.

[28]Corke, T.C., *Design of Aircraft*, Upper Saddle River, New Jersey, 2003, Chaps. 2-8.

[29]Roxburgh, Gordon, "Concorde SST," *Concorde*. http://www.concordesst.com/.

[30]Liu, F. and Sirignano, W.A., "Turbojet and Turbofan Engine Performance Increases through Turbine Burners," *Journal of Propulsion and Power*, Vol. 17, No. 3, May-June 2001, pp. 695-705.

[31]"Space Shuttle Coordinate System," NASA Shuttle Reference Manual: 1988.
http://science.ksc.nasa.gov/shuttle/technology/sts-newsref/sts_coord.html#vertical_tail.

[32]"X-29 Fact Sheet," NASA Dryden Flight Research Center: 2008.
http://www.nasa.gov/centers/dryden/news/FactSheets/FS-008-DFRC.html

[33]Strykowski, P.J., Krothapalli, A., Forliti, D.J., "Counterflow thrust vectoring of supersonic jets," *AIAA Journal*, Vol. 34, No.11, 1996, pp. 2306-2314.

[34]Pantelakis, S., Kyrsanidi, A., El-Magd, E., Dunnwald, J., Barbaux, Y., Pons, G., "Creep resistance of aluminum alloys for the next generation supersonic civil transport aircrafts," *Theoretical and Applied Fracture Mechanics*, Vol. 31, 1999, pp. 31-39.

[35]Durston, D.A., “A Preliminary Evaluation of Sonic Boom Extrapolation and Loudness Calculation Methods,” NASA CP 10133, 1994, Proceedings of High-Speed Research: Sonic Boom, Vol. 2, NASA Ames Research Center, May 12-14, 1993, pp. 301-323.

[36]Thomas, C.L., “Extrapolation of Wind-Tunnel Sonic Boom Pressure Signatures Without Use of a Whitham F-Function,” NASA SP-255, 3rd Conference on Sonic Boom Research, NASA HQ, October 29-30, 1970, pp. 205-217.

[37]Thomas, C.L., “Extrapolation of Sonic Boom Pressure Signatures by the Waveform Parameter Method,” NASA TN D-6832, June 1972.

[38]Needleman, K.E., Darden, C.M. and Mack, R.J., “A Study of Loudness as a Metric for Sonic Boom Acceptability,” AIAA Paper 91-0496, AIAA 29th Aerospace Sciences Meeting, Reno, NV, January 7-10, 1991.

[39]Plotkin, K.J., “Calculation of Sonic Boom from Numeric Flow Field Solutions: MDBoom Version 2.2, Wyle Research Report WR 92-14,” Wyle Laboratories, July 1992 (prepared for Douglas Aircraft Company, Long Beach, CA under Agreement number AS-25254-C, McDonnell Douglas Report Number MDC 92K0370).

[40]Seebass, R., “Sonic Boom Minimization,” RTO AVT Course – Fluid Dynamics Research on Supersonic Aircraft, Rhode-Saint-Genese, Belgium, May 25-29, 1998.

[41]Salvetti, A. and Seidman, H., “Noise and Sonic Boom Impact Technology,” PC Boom Computer Program for Sonic Boom Research: Program Users/Computer Operations Manual, Air Force Systems Command, October 1988.

[42]Zha, G.-C., "Toward Zero Sonic-Boom and High E±ciency Supersonic UAS: A Novel Concept of Supersonic Bi-Directional Flying Wing." US Air Force Academic Outreach UAS Symposium, Grand Forks, ND, Aug. 4-6, 2009.

[43]Zha, G.-C., Im, H, Espinal, D. "Toward Zero Sonic-Boom and High Efficiency Supersonic Flight, Part I: A Novel Concept of Supersonic Bi-Directional Flying Wing.", AIAA Paper 2010-1013, 48th AIAA Aerospace Sciences Meeting, Orlando, FL, Jan.4-6, 2010.

[44]Durston, D. A. , \ Sonic Boom Extrapolation and Sound Level Prediction." Unpublished Document, NASA Ames Research Center, Sept. 2009.

Flight Stage	Weight (lb)
Max Take-Off	81,232
Start-up & Take-Off	79,202
Climb & Accel to Cruise	74,608
Cruise to Destination	58,093
Loiter	57,018
Landing	55,592

Table 1. Weight of SB-8060-3 at different flight stages

Dimension	SBiDir-FW (supersonic mode)	Concorde[29]
Total Length (m)	60.0	61.7
Wing Span (m)	22.6	25.6
Fuselage Max. Height (m)	1.80	3.32

Table 2. Geometric characteristics comparison between SBiDir-FW and Concorde

Specifications	SBiDir-FW	Concorde[0]
Cruise Speed	Mach 1.6	Mach 2.0
Range (nmi)	2,000	3,900
Payload (passengers)	70	100
Take-off field length (ft)	2,473	11,800
Fuel Efficiency (passenger mi/lb)	5.93	2.13
Cruise L/D	7.50	7.14
Overpressure (psf)	0.90	1.94

Table 3. Performance comparison between SBiDir-FW and Concorde

Geometric Characteristic	Subsonic	Supersonic
Span (m)	60.0	22.6
Aspect Ratio	7.28	1.03
Sweep Angle (Length Average)	20.0°	70.0°
Airfoil Thickness	3%	8%

Table 4. Geometric characteristics comparison between modes

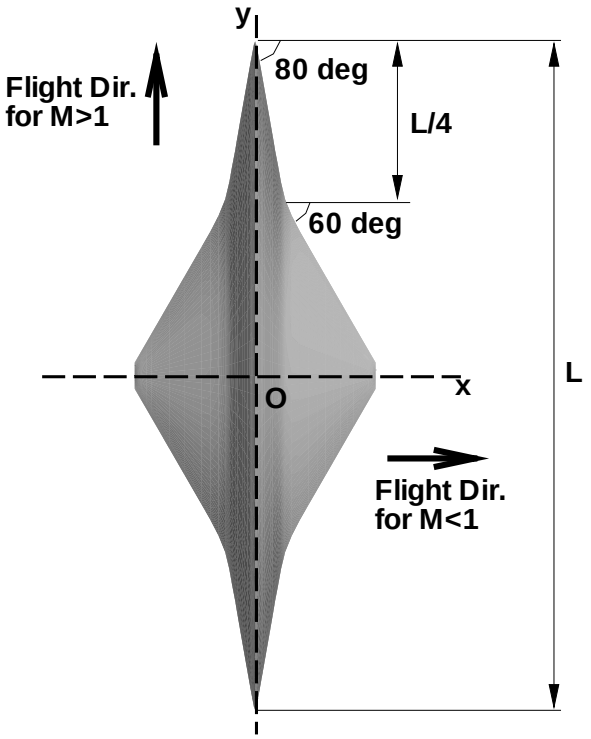

Figure 1 – Planform shape showing LE sweep angles, axes of symmetry and flight directions for subsonic (M<1) and supersonic (M>1) modes.

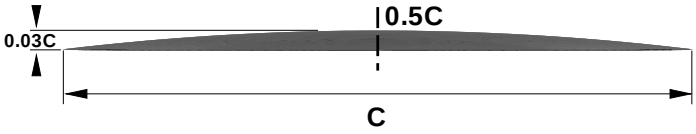

Figure 2 – Airfoil section for supersonic mode, symmetric about the 50% chord length. Suction surface is a circular-arc and pressure surface is a flat plate. Maximum thickness is 3% at the 50% chord length.

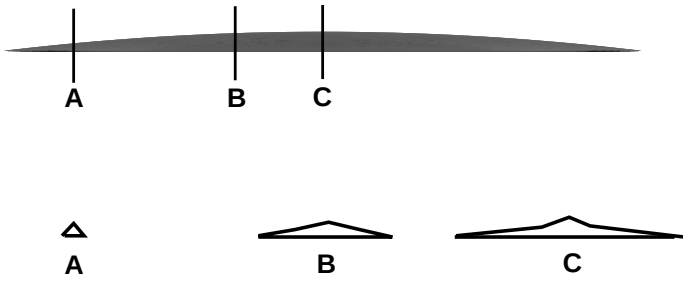

Figure 3 – Airfoil sections in subsonic mode close to the wingtip (A), between wingtip and center (B) and at the axis of symmetry (C).

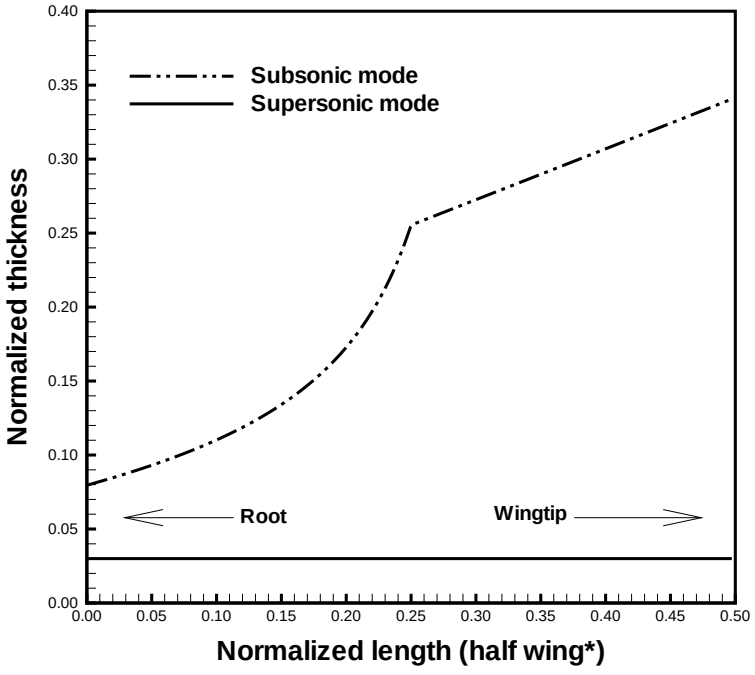

* For half wing 0.00 is the root and 0.50 is the wingtip

Figure 4 – Thickness distribution for subsonic and supersonic modes for half wing.

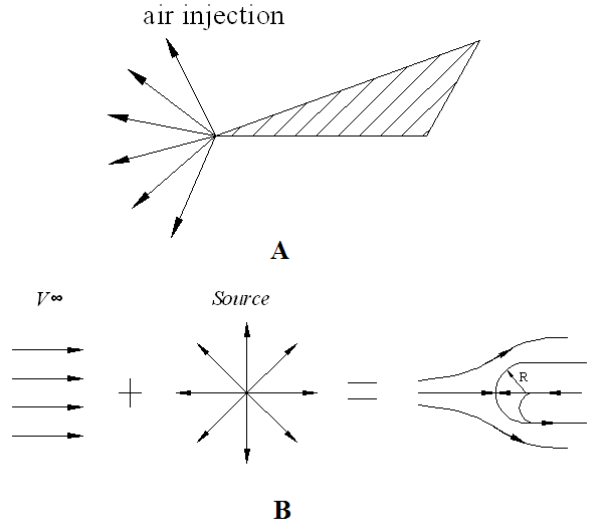

Figure 5 – LE treatment using radial air injection (A) that when combined with a uniform creates a blunt body flow of radius R (B).

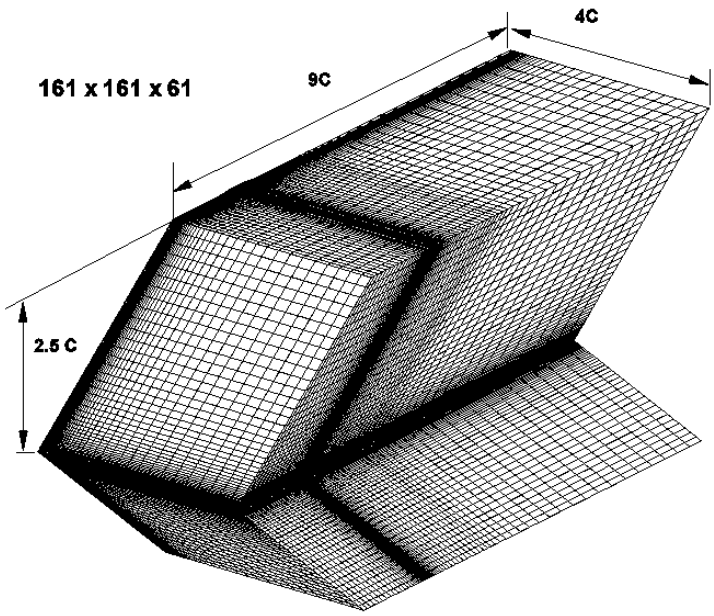

Figure 6 – 3D inclined mesh used to perform CFD analysis of SB-8060-3 (only half planform). Angle of incline depends on cruise Mach number. Mesh created for sonic boom measurements.

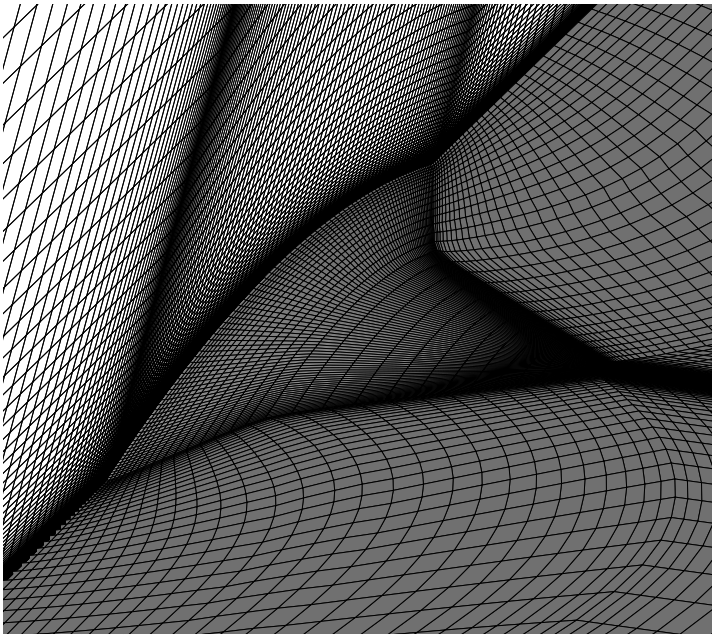

Figure 7 – Surface mesh for CFD analysis of half planform of SB-8060-3.

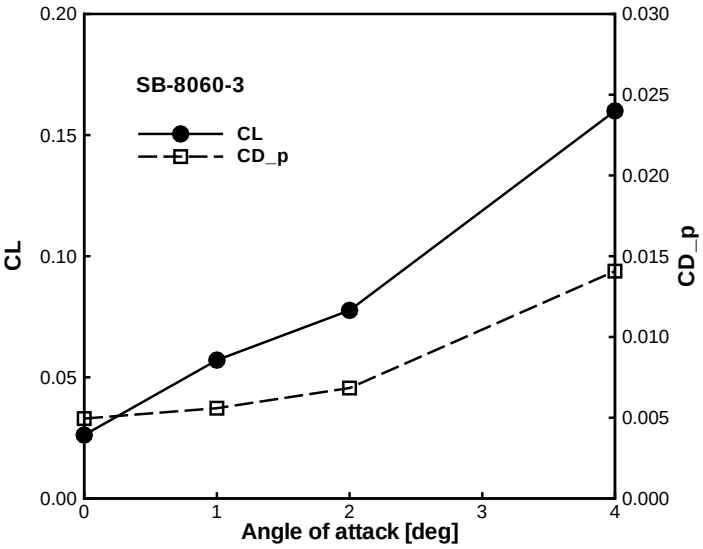

Figure 8 – Plot of C_L and C_{Dp} with respect to AoA for SB-8060-3 for a cruise Mach number of 1.6.

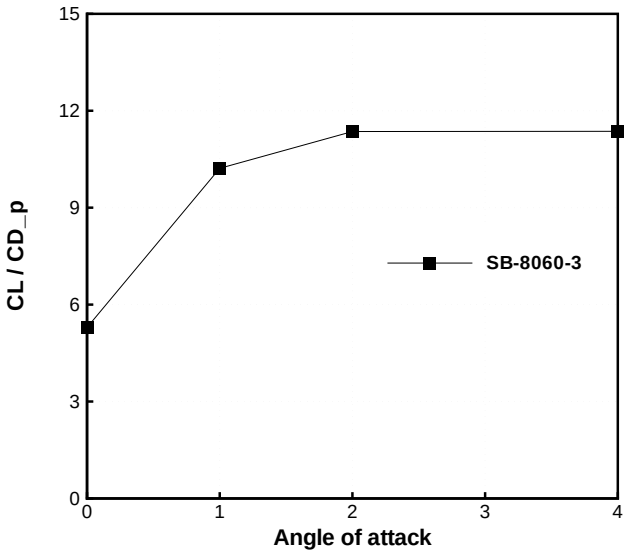

Figure 9 – Plot of C_L/C_{Dp} with respect to AoA for SB-8060-3 for a cruise Mach number of 1.6 to help estimate the ratio of L/D.

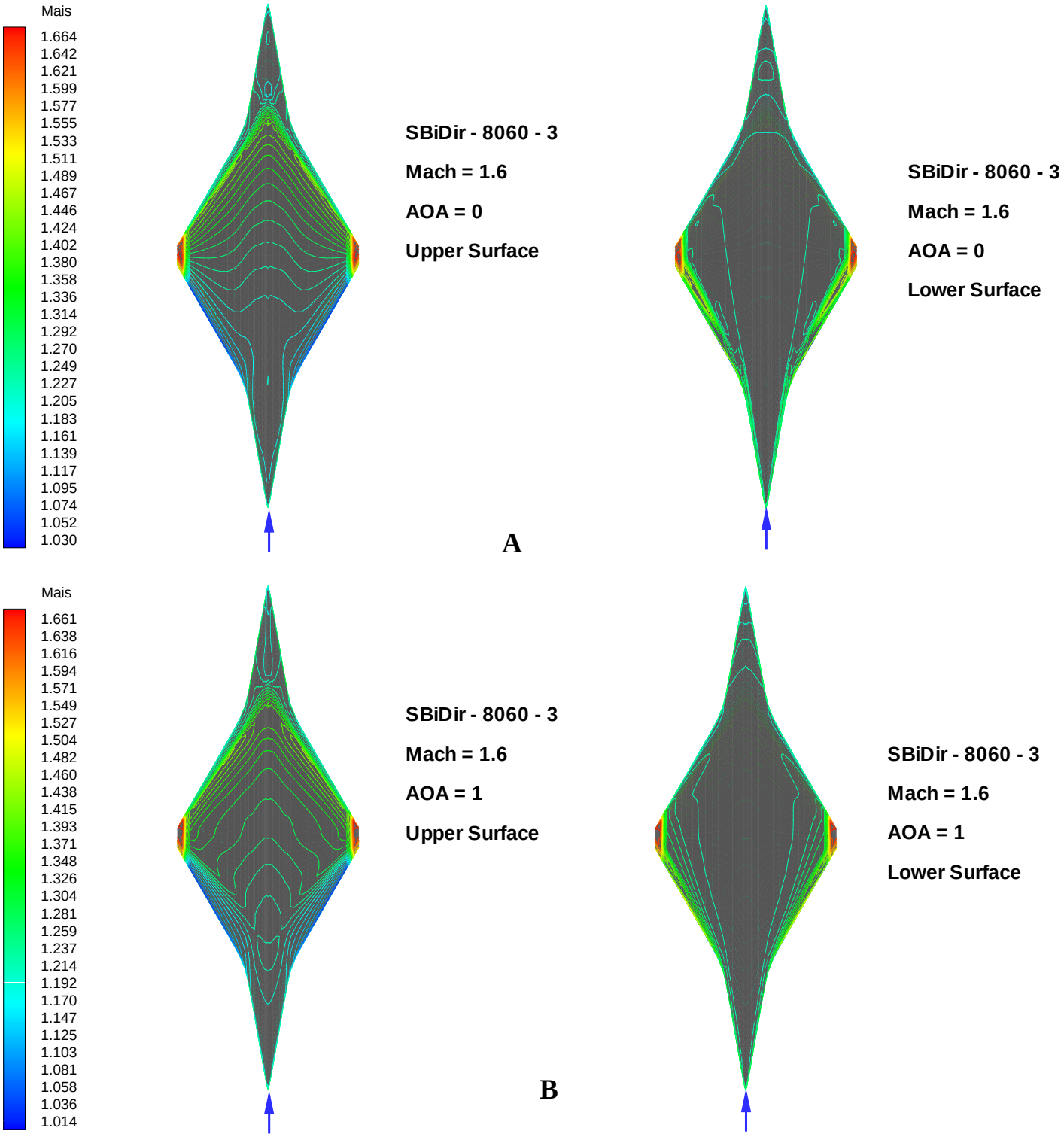

Figure 10 – Isentropic Mach contours on the upper and lower surface of SB-8060-3 exhibiting a strong shock on the top surface and an almost uniform distribution at the bottom surface for AoA of 0^{O} (A), 1^{O} (B), 2^{O} (C) and 4^{O} (D).

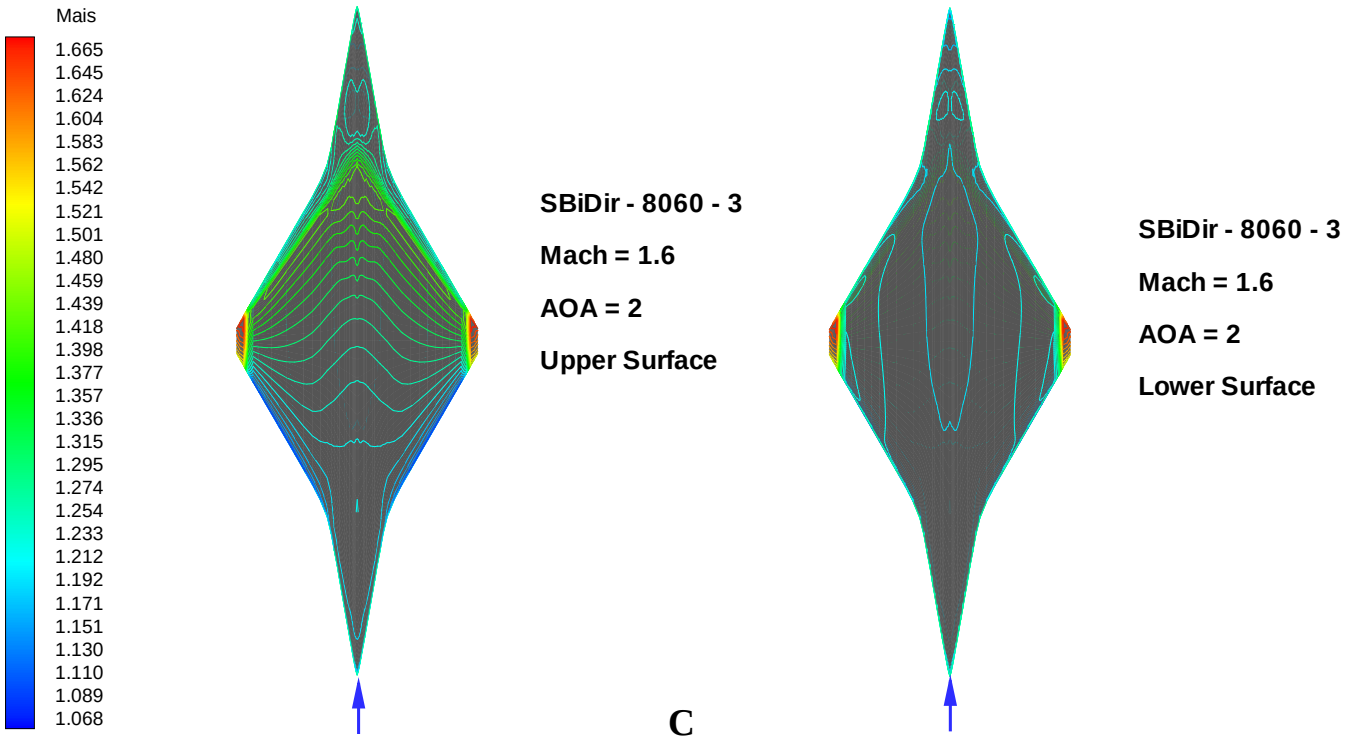

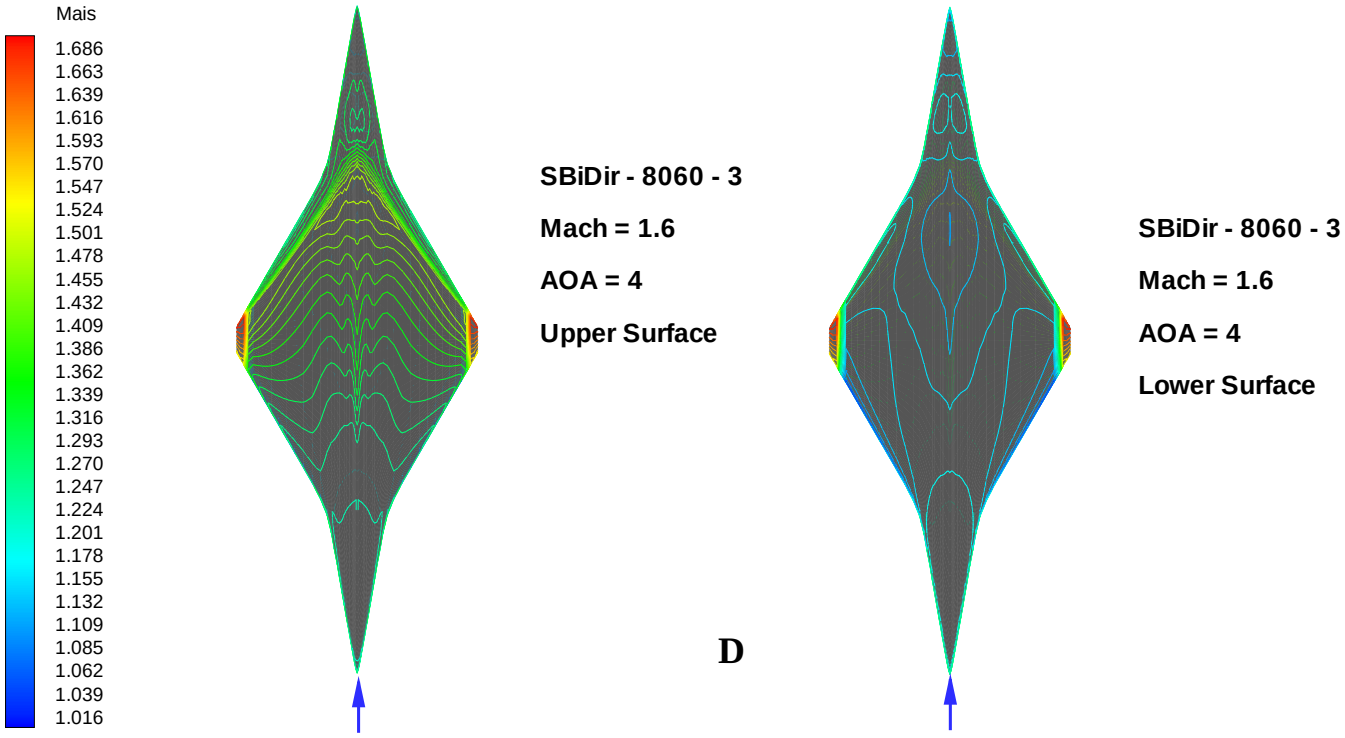

Figure 10 (Cont'd.) – Isentropic Mach contours on the upper and lower surface of SB-8060-3 exhibiting a strong shock on the top surface and an almost uniform distribution at the bottom surface for AoA of 0^{O} (A), 1^{O} (B), 2^{O} (C) and 4^{O} (D).

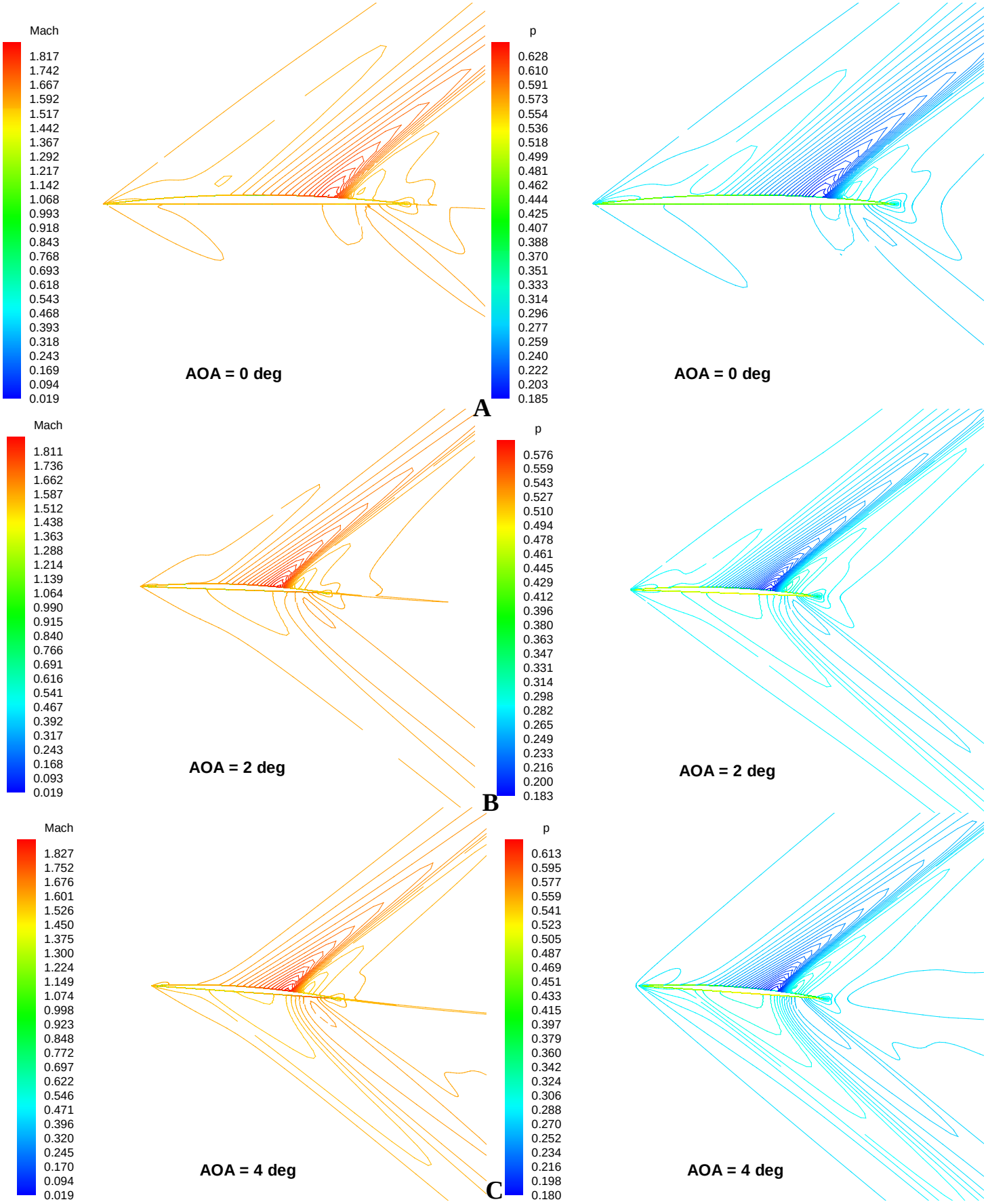

Figure 11 – Mach (left) and pressure (right) contours for SB-8060-3 exhibiting a strong shock on the top surface and a weaker shockwave at the bottom surface for AoA of 0^{O} (A), 2^{O} (B) and 4^{O} (C).

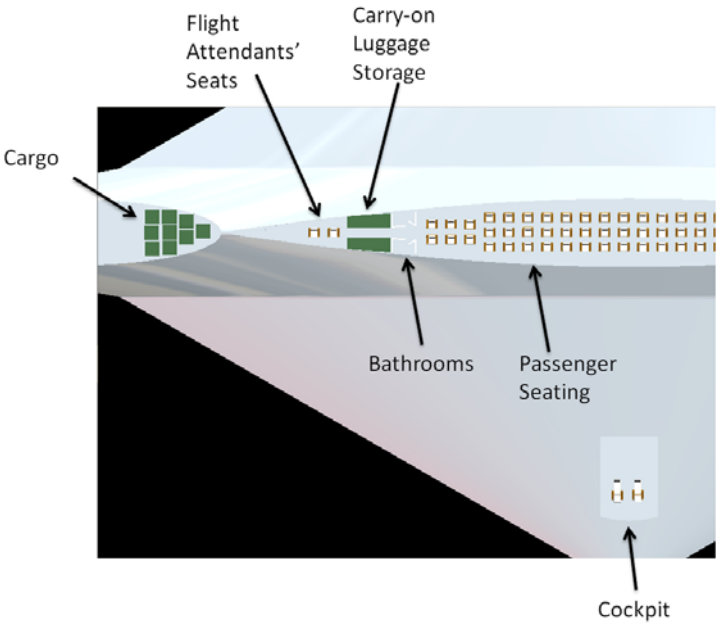

Figure 12 – Detailed layout of passenger cabin, cargo and cockpit and its corresponding locations on SB-8060-3.

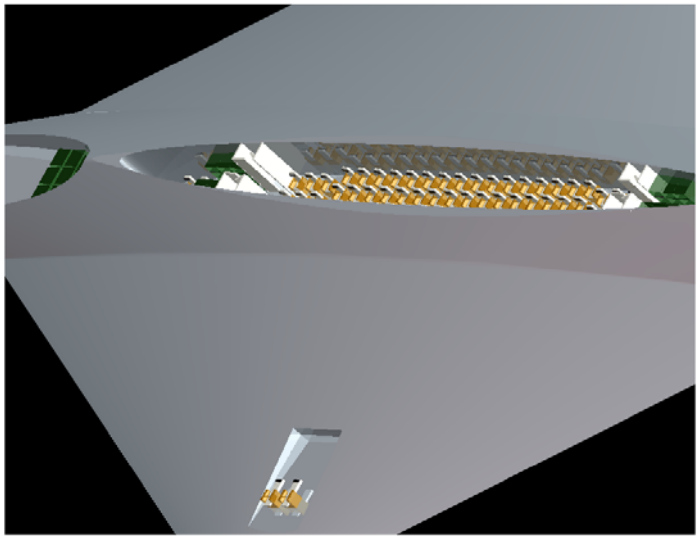

Figure 13 – Orthographic view of interior layout.

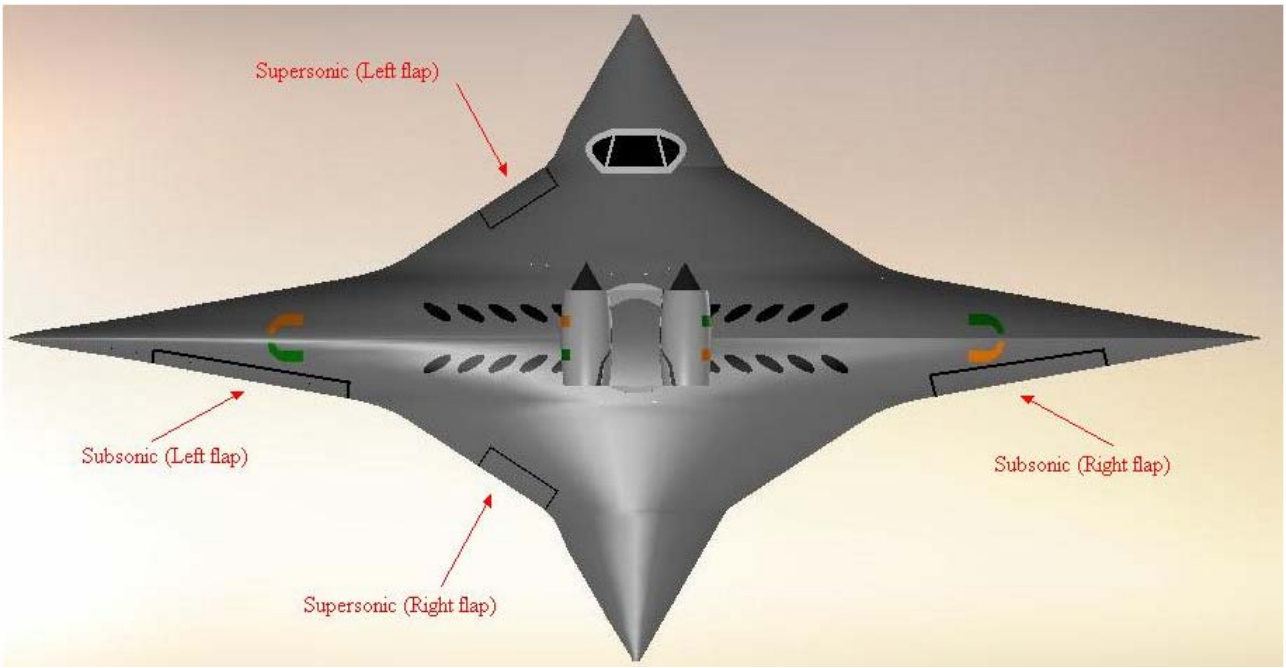

Figure 14 – Location of control surfaces supersonic and subsonic modes. Also, winglets (not shown) will be used for subsonic flight and canards (not shown) for supersonic flight to aid control and stability.

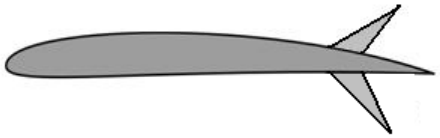

Figure 15 – Sketch of split flap required for controlling the six degrees of freedom of SBiDir-FW. Top and bottom flaps move independently of each other.

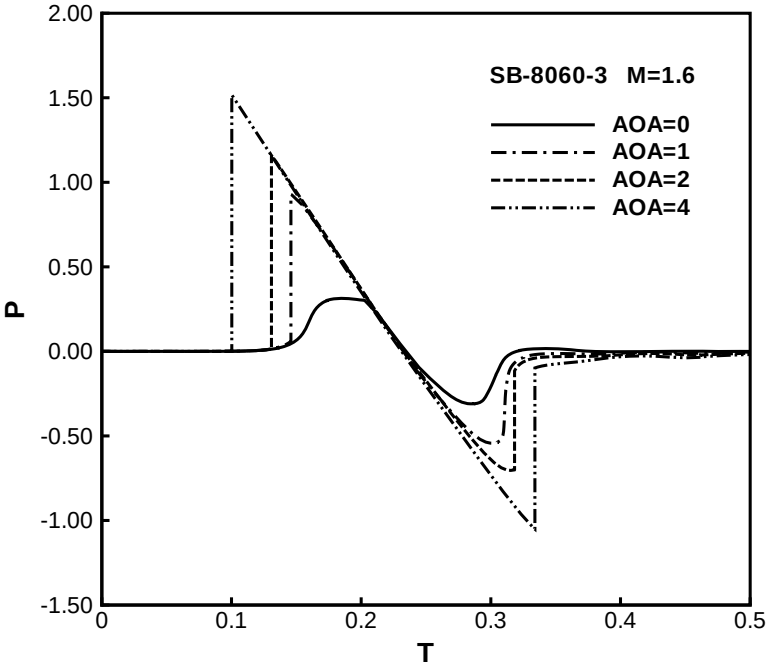

Figure 16 – Overpressure on ground due to sonic boom propagation for SB-8060-3 flying at Mach 1.6 at an altitude of 60,000 ft for different AoA..

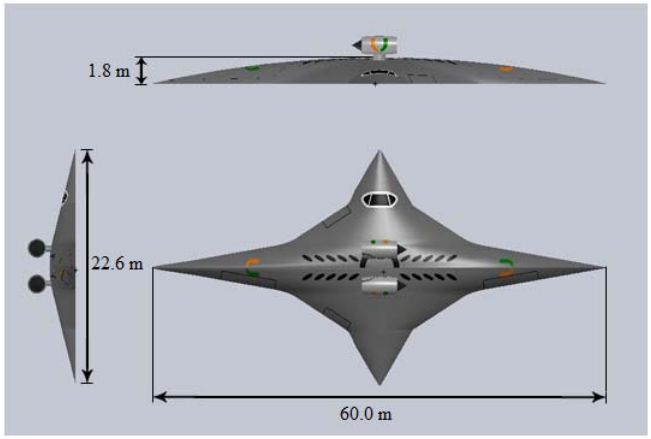

Figure 17 – Final dimensions of a SBiDir-FW for an aircraft with capacity of 70 passengers.

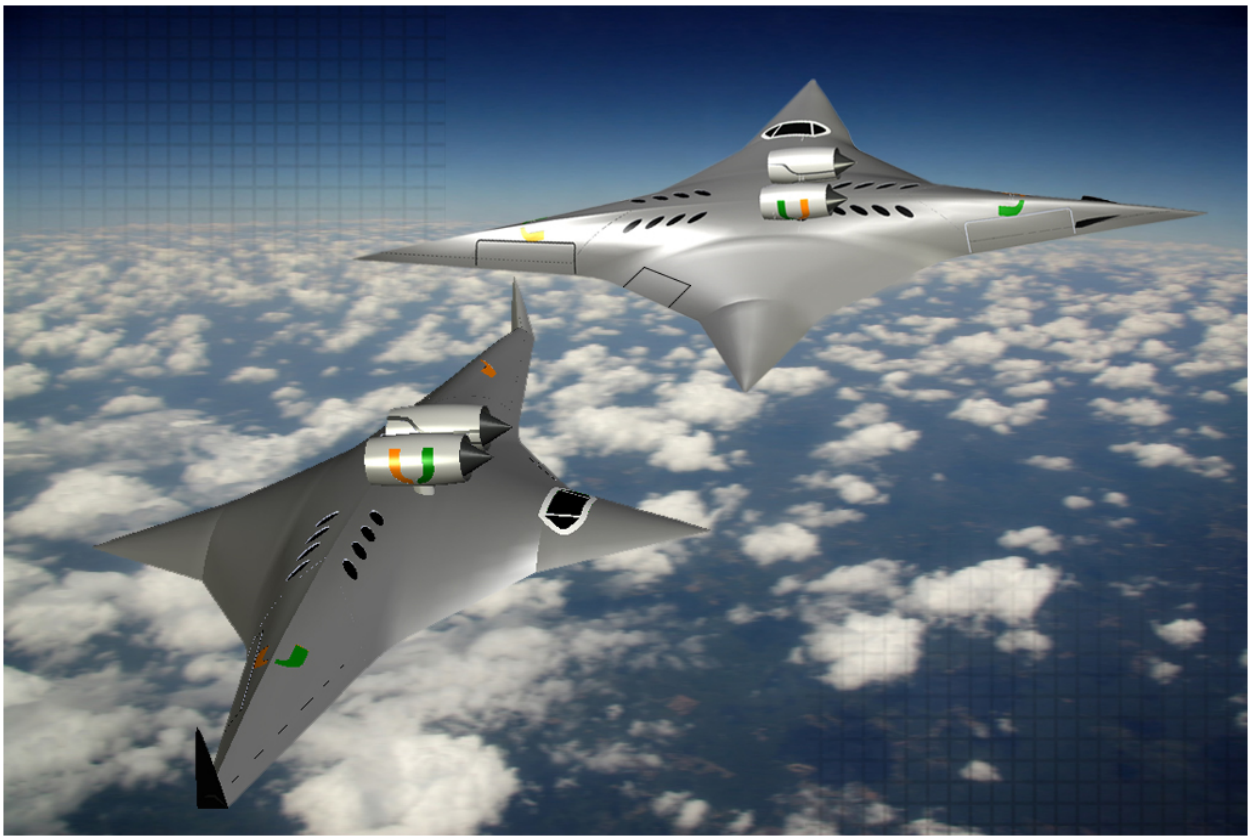

Figure 18 – Rendition of both subsonic (bottom left) and supersonic (top right) modes for SBiDir-FW. The wing is flying from left to right. The subsonic mode fashions winglets at the wingtips while the supersonic mode shows small canards on the front. Both modes show the two engines in front of the center to improve static margin.